Thermochimica Acta 492 (2009) 95–100

Contents lists available at ScienceDirect

Thermochimica Acta

journal homepage: www.elsevier.com/locate/tca

Calorimeter chip calibration for thermal characterization of liquid samples

E. Iervolino[a,*], A.W. van Herwaarden[a], P.M. Sarro[b]

[a] Xensor Integration, Distributieweg 28, 2645 EJ Delfgauw, The Netherlands[1]
[b] Delft University of Technology, DIMES, Feldmannweg 17, 2628 CT, The Netherlands

ARTICLE INFO

Article history:
Available online 3 May 2009

Keywords:
Calorimeter chip
Microfluidic
Thermal conductivity
Thermal diffusivity
Thermopile

ABSTRACT

We present the fabrication and calibration of a novel calorimeter chip for thermal characterization of liquid samples. The device we present consists of two chips glued on top of each other. Both chips consist of a freestanding SiN membrane with a poly-Si heater and thermopile in the center of the membrane. The calibration liquid is contained between the two SiN membranes. The calibration of the calorimeter chip is necessary to measure the thermal properties of liquid samples under test. We utilized water–alcohol mixtures for the calibration. A resolution of 0.02 mW/K m and 0.001 mm^2/s has been obtained for thermal conductivity and thermal diffusivity measurements, respectively.

1. Introduction

Calorimetry is the science of measuring the heat of chemical reactions or physical changes. A calorimeter device is also very well suited for measuring thermal properties of sample materials. Thermal conductivity and thermal diffusivity of sample materials have been measured [1–6] using calorimeter chips. These thermal properties are function of the temperature, and a device made to measure these properties has to provide enough thermal isolation towards the ambient.

Indeed, the performance and the reliability of thermal-property sensors are often limited by the poor thermal isolation of their liquid cells. In particular, calorimeters with a glass micro-fluidic chamber [1–5] are not suitable for thermal diffusivity measurements. The proximity of the heater to the thermopile is a limiting factor in such calorimeters as the effective thermal diffusivity of the membrane-sample system is dominated by the thermal diffusivity of the membrane. In [6] a CMOS sensor is proposed for measuring the thermal diffusivity of liquid samples dropped directly onto the device. Another external factor that can influence the measurements of the thermal properties of the sample under test is the frequency of the applied signal. The 3-ω method is commonly considered for the measurements of the frequency dependent complex heat capacity. Another method, temperature wave analysis (TWA), is used to obtain the thermal diffusivity of solid sample by measuring phase and amplitude of a thermal wave transmitted through the sample itself [7]. In this technique an oscillating heat flow $P_0\,cos(\omega t)$ is applied to one side of the plate-like sample and the oscillating temperature $T_0\,cos(\omega t+\varphi)$ is detected on the other side. A recent work [8] used the same principle shown in [7] to measure the complex heat capacity $C(\omega)$ with a two-channel calorimeter.

The aim of this work is to present the experimental results obtained with the calibration of the device XI-318-9. Thanks to the good thermal isolation towards the ambient the device is suitable for measuring both thermal diffusivity and thermal conductivity of liquid samples. The output signals of the device at 1 Hz and 10 mHz are put in relation with the thermal diffusivity and conductivity of the sample under test, respectively. In order to perform the device calibration we used demineralized (demi) water; isopropanol (IPA) and water–methanol mixtures at different methanol concentrations.

2. Device description

2.1. Sensor description

The thermal conductivity is the property of a material that indicates its ability to conduct heat. The thermal diffusivity is a measure of how fast the heat is transferred through the material.

The calorimeter chip [9] has been used to measure both the thermal diffusivity and the thermal conductivity of liquid samples. The device consists of two stacked calorimeter chips. Both chips have a heater and a thermopile on top of a freestanding 2 μm thick silicon nitride (SiN) membrane. The heater is made from p-type polycrystalline silicon (poly-Si) and is located in the center of the membrane. The thermopile consists of 36 p-polySi/n-polySi thermocouples. The hot junctions of the thermopile are located on the freestanding membrane at 20-μm distance from the heater whereas the cold junctions are located on the rim of the silicon chip. The large thermal mass and the good thermal conductance of the silicon rim keep the cold junctions at room temperature while

* Corresponding author. Tel.: +31 0 15 2578040; fax: +31 0 15 2578050.
E-mail address: eli@xensor.nl (E. Iervolino).
[1] http://www.xensor.nl.

0040-6031/$ – see front matter © 2009 Elsevier B.V. All rights reserved.
doi:10.1016/j.tca.2009.04.021

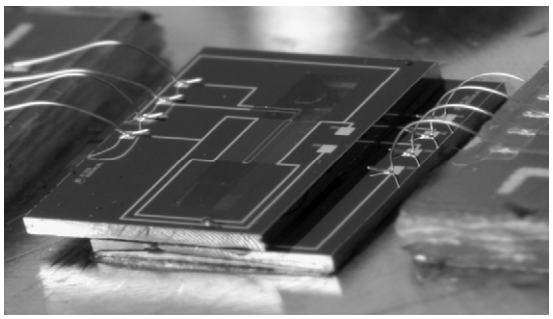

Fig. 1. Photograph of the two chips which form the device XI-318-9. The transparent membranes are 3.8 mm × 0.8 mm (top chip) and 2 mm × 0.8 mm (bottom chip).

the membrane, that has a low thermal conductance, allows the hot junctions to follow the rise in temperature of the heater. The thermopile and heater resistances of both chips are designed to have the same resistance, i.e. about 50 and 6.6 kΩ, respectively.

The liquid sample is isolated between these membranes, which are 300 μm apart. Fig. 1 shows a photograph of the calorimeter chip. The general idea is to create a liquid volume that is mainly contained between the thin SiN membranes. In this way, a good thermal isolation towards the ambient is obtained. The device is also glued on top of an aluminum (Al) block with a large thermal mass to reduce the thermal drift. An exploded view of the device is presented in Fig. 2a where the two chips glued on top of each other, the Al block and the two Teflon tubes are visible. The Al block has openings aligned to the inlet and outlet of the chip. The liquid sample is injected into the device via a syringe through a Teflon tube that is screwed into the aluminum block inlet. The liquid sample goes out of the device through the other Teflon tube. However the device can also be used in-line in an experimental set-up, although the best measurement quality is obtained when the flow is (temporarily) stopped.

In Fig. 2b we show the other side of the measurement set-up. We can see the two holes used to screw the Teflon tubes. They correspond to the inlet and outlet of the chip. A third hole in between the two Teflon tubes (where the arrow is pointing) has been made to avoid a hermetical seal of the cavity underneath the membrane of the bottom chip. The chip is not visible in Fig. 2b as it is glued on the other side of the Al block.

In order to perform the measurements, the device is inserted inside a CTS oven T-65/50. The input signal to the device is generated by a lock-in amplifier (SR830) also used to measure the output signal of the device.

2.2. Sensor characterization

The relative Seebeck coefficient $\alpha_{sc,n} - \alpha_{sc,p} = \alpha_{sc}$ of the p-polySi/n-polySi thermocouple is about 300 μV/K at 293 K so, the nominal sensitivity of the thermopile is about 11 mV/K.

Table 1
Comparison of liquid calorimeter chips.

Chip parameters in water	NCM-9924 [5]	Köhler [3,4]	Zhang [1,2]	XI-318-9 [9]
Transfer [V/W]	1.0	0.75	0.94	11
Volume [μl]	30	2	0.1	1
Volume transfer [μl V/W]	30	1.5	0.59	11
Thermal resistance [K/W]	10	25	200	850
Output resistance [kΩ]	50	8	200	50
Time constant [s]	0.7	5	0.1	0.5
Noise [μV]	2.5	2.5	0.1	2.5
NEP [μW]	2.5	3	0.1	0.2

The transfer of the thermopile was measured varying the power dissipated in the heater. When the device is filled with non-flowing water the transfer is about 11 V/W. With flowing water the transfer decreases. For 10 μl/min flow the decrease is 2.5% and at 500 μl/min the transfer is nearly halved.

A thermal resistance of 1 kK/W is calculated from the values of the measured transfer and the nominal thermopile sensitivity.

The time constant is measured applying heat pulses to the heater and measuring the response of the thermopile. A value of 0.5 s is found when the device is filled with non-flowing water

2.3. Comparison with other liquid calorimeter chips

In Table 1 we compared a few liquid calorimeter chips with the chip XI-318-9. The transfer in V/W of the chip is much higher than previously reported chips, while the volume is generally lower. For use with experiments where the signal is generated by a volumetric reaction, the power produced in a much smaller volume is proportionally lower. This, however, is to some degree compensated by a much higher transfer, so that the sensitivity of the device for volumetric reactions, such as enzyme conversions, is comparable. Only, much less chemicals are needed, which can be an advantage when the chemicals are expensive or scarce. The smaller volume also has advantages in refreshing time. It is important also to compare the capability of the devices in rejecting the noise. We measured a noise of 2.5 μV in non-flowing water. It is interesting to note that the noise is about the same for all the devices except for the chip present by Zhang [1,2]. He measured a noise about ten times lower. The noise he presented is measured with glucose at a flow rate of 15 nl/s. Though Zhang measured a lower noise the noise equivalent power (NEP) is comparable with what we calculated. This is because of the low transfer he measured.

3. Fabrication

The chips are made using a thin-film bulk-micro-machining process. A schematic flow chart of the processing steps is depicted in

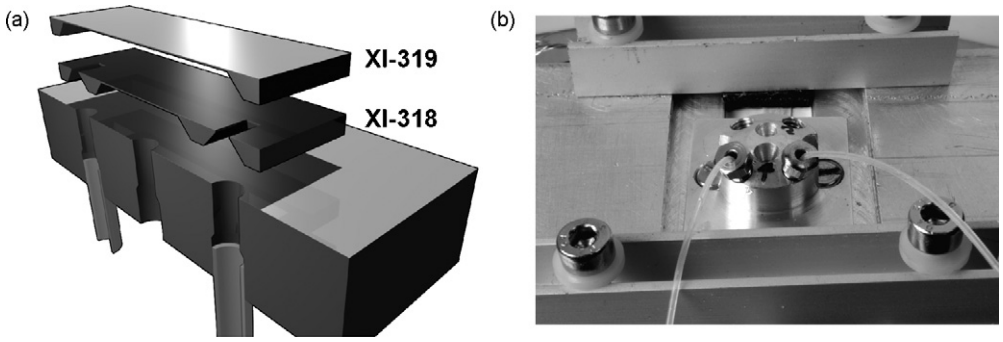

Fig. 2. (a) Exploded view of the device XI-318-9. It is shown: the two stacked chips (XI-318 XI-319); the Al block; the Teflon tubes. Not to scale. (b) Bottom side of the Al block.

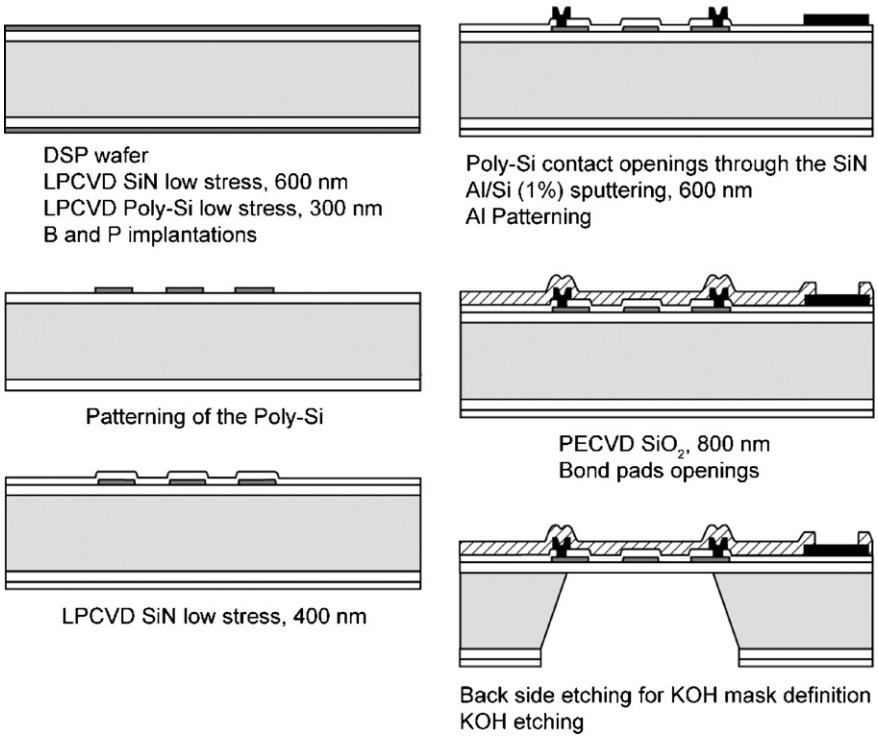

Fig. 3. Calorimeter chip process flow.

Fig. 3. The device is fabricated on a 300 μm thick<1 0 0> p-type double side polished (DSP) silicon wafer. The first step is a low-pressure chemical vapor deposition (LPCVD) of low-stress SiN [10]. Then, a 300 nm thick LPCVD low-stress poly-Si layer is deposited on the top of the SiN. The poly-Si layer is implanted, using photoresist masks, with phosphorus and boron in order to make low-resistive n-type and p-type regions (50 and 75 Ω/sq, respectively). After implantation, the poly-Si is patterned and covered by a 400 nm thick LPCVD SiN. Contact openings for the poly-Si are etched through the SiN layer and a 600 nm thick Al/Si (1%) layer is deposited by RF sputtering. After the patterning of the Al layer by dry etching, a scratch protection layer of 800 nm of SiO_2 is deposited by plasma-enhanced chemical vapor deposition (PECVD). In order to open the bond pads, a dry etching of the silicon oxide stopping on the Al layer is then performed.

The process on the backside of the wafer consists of the SiN layer patterning followed by the etching of the Si substrate in a potassium hydroxide (KOH) solution to release the membrane. After the dicing step, the chips are ready for assembly.

4. Calibration procedure

4.1. Thermal properties versus frequency

The measurement of the thermal properties of a certain substance can be influenced by external variables like the ambient temperature and the frequency. When a substance is in a phase transition region (i.e. from solid to liquid, from liquid to gas, etc.) thermal energy is used to effect the phase change. The relaxation time of this conversion can cause the frequency dependence of the measurement of the thermal properties of the substance [7]. On the other hand Morikava and Hashimoto [11] found that the measurement is not frequency dependent away from the phase transition regions of a substance.

We are interested in determining the thermal properties of samples in their liquid phase, away from their phase transition region. For that reason the choice of the measurement frequencies is dictated only by practical reasons.

4.2. Calibration method

For the calibration procedure we used a lock-in amplifier to apply a sinusoidal signal at frequency ω to the heater. The heater sends heat waves (or temperature waves as some prefer to say) through the liquid sample to the thermopile on the opposite membrane. The frequency of the heat wave P is twice the heater voltage frequency because

$$P(\omega) = \frac{U_h(\omega)^2}{R_h} \tag{1}$$

where R_h is the heater electrical resistance and U_h is the heater voltage. The thermopile output voltage can be written as

$$U_{out}(\omega) = N\alpha_{sc}T(\omega) = N\alpha_{sc}P(\omega)Z_{th}(\omega) \tag{2}$$

where N is the number of thermocouples, α_{sc} is the Seebeck coefficient of the thermopile and Z_{th} is the thermal impedance of the device and the liquid sample. The output voltage of the thermopile will be a sinusoidal signal with the same frequency 2ω as P and with an initial phase $\varphi \neq 0$. From Eq. (2) we see that the product of the thermal impedance with the heat P equals the temperature elevation T of the hot junction of the thermopile respect to the temperature of the cold junction of the thermopile. The temperature of the cold junction of the thermopile can be assumed to be the ambient temperature T_{amb} and it is frequency independent while the temperature of the hot junction is frequency dependent. The behavior of T can be calculated solving the heat diffusion equation of the heat flow through the liquid sample

$$\begin{cases} \nabla^2 T\alpha = \dfrac{\partial T}{\partial t} & \textit{in the sample} \\ \nabla^2 T\alpha_s = \dfrac{\partial T}{\partial t} & \textit{in the substarte} \end{cases} \tag{3}$$

where T is the temperature elevation above T_{amb}, α is the thermal diffusivity of the liquid sample and α_s is the thermal diffusivity of the substrate. To give an approximated idea of the behavior of our device, we can take the same assumptions as Hashimoto et al. [7]: the heat is flowing in one dimension; the substrate is semi-infinite so that $T(x \to -\infty, t) = T(x \to +\infty, t) = 0$ at the infinity; $kd > 1$ with d the value of the path covered by the heat wave (300 μm in our device) and $k = \sqrt{(\omega/2\alpha)}$. Under these assumptions the temperature elevation T above T_{amb} is approximately given by [7]

$$T(d,t) = \frac{\sqrt{2}q_0 kKe^{-kd}}{(kK + k_s K_s)^2} e^{j(\omega t - kd - (\pi/4))}, \quad kd > 1 \tag{4}$$

where K and K_s are the thermal conductivities of the sample and the substrate, respectively, $k_s = \sqrt{(\omega/2\alpha_s)}$ and $q_0 e^{j\omega t}$ is the heat wave per unit area. Using Eq. (4) we can approximate Eq. (2) as follows:

$$U_{out}(\omega) = N\alpha_{sc} \frac{\sqrt{2}q_0 kKe^{-kd}}{(kK + k_s K_s)^2} e^{j(\omega t - kd - (\pi/4))}, \quad kd > 1 \tag{5}$$

If we neglect the influence from the substrate (in our case a very thin membrane and air) we end up with the following equation:where $P_0 = Aq_0$ is the amplitude of the heat wave (measured in W), A is the area crossed by the heat flow. The term d/KA in Eq. (6) is the thermal resistance (measured in K/W) of the liquid sample:

$$U_{out}(\omega) = N\alpha_{sc} P_0 \frac{d}{KA} \frac{\sqrt{2}e^{-kd}}{kd} e^{j(\omega t - kd - (\pi/4))}, \quad kd > 1 \tag{6}$$

$$R_{th} = \frac{d}{KA} \tag{7}$$

Using Eq. (7), U_{out} is approximately given by

$$U_{out}(\omega) = N\alpha_{sc} P_0 R_{th} \frac{\sqrt{2}e^{-kd}}{kd} e^{j(\omega t - kd - (\pi/4))}, \quad kd > 1 \tag{8}$$

Eq. (8) shows the DC contribution ($N\alpha_{sc}P_0R_{th}$) and, the frequency dependent attenuation ($\sqrt{2}e^{-kd}/kd$) and phase $-kd - (\pi/4)$ of U_{out}. These calculations are made to give a general idea of the relations that exist between the thermal properties of the sample under test and the measured signals. They do not describe our device. Indeed, because of the 3D structure of the device a more correct calculation should include all the three directions of the heat flow. Furthermore the substrate is not semi-infinite.

A theoretical analysis of the device is beyond the purpose of this paper. Our purpose is to obtain the relation between the measured signals and the thermal properties of the liquid sample under test (i.e., the calibration curves of the device).

In order to obtain the calibration curves we studied the output signal in terms of its amplitude and phase.

4.2.1. Thermopile voltage amplitude

We applied to the heater an AC voltage. We varied the frequency from 10 mHz to 1 Hz keeping the amplitude constant. In Fig. 4 we show the amplitude of the thermopile voltage versus frequency for water and IPA. Experimentally we found that both the amplitudes of the curves for water and IPA decrease with frequency.

As we can see from Fig. 4, at 10 mHz, the curve obtained for water (thermal conductivity of 0.598 W/K m) is below the curve obtained with IPA (0.14 W/K m). The temperature increase at the opposite membrane of the heater is lower with the water than with IPA as, at lower frequency (10 mHz) the lateral cooling of the water is better than by IPA, relative to the vertical heat transfer from the heater to the thermopile at the opposite membrane. At such low frequency, 10 mHz, the behavior is very much like that at DC and the thermal diffusivity of the sample does not play a significant role. At higher frequency (1 Hz) the thermal horizon for thermal waves in IPA ($1/k_{IPA}d$) is smaller than in water ($1/k_{H_2O}d$) and the lateral cooling starts to lose its effect. This explains why the amplitude for

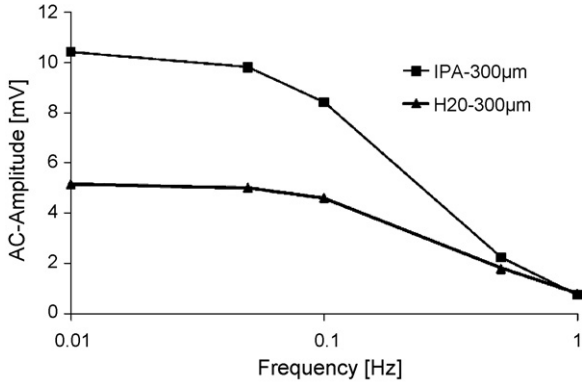

Fig. 4. AC amplitude of the thermopile voltage for two liquid samples (water and IPA) with a heating power of 1.5 mW_{p-p}. Measurements are done at 30 °C across a 300-μm distance.

IPA starts to fall below that of water. In Fig. 4 is it visible that this effect starts at 1 Hz. Measurements at 5 Hz has been done to confirm this behavior but they are not reported in present paper.

Our purpose is to make a relation between U_{out} and the thermal conductivity of the liquid sample. For that reason, to make the calibration curve, for thermal conductivity measurements, we considered the amplitudes of the thermopile voltage measured at 10 mHz. We did not perform measurement at DC because AC measurements allowed us to use a low-noise measurement set up and at 10 mHz the behavior is very much like that at DC.

To compare results at different frequencies, a frequency dependent calibration factor has to be calculated, solving Eq. (3). But, as we already mentioned, it is not our intention to make a theoretical analysis of the device.

4.2.2. Thermopile voltage phase

Information on the thermal diffusivity of the liquid sample are obtained by measuring the phase shift between $U_{out}(\omega)$ and the heater voltage as the heat waves are not only attenuated by the liquid sample but also delayed. As example we report the measurements obtained with water (0.143 mm^2/s) and IPA (0.068 mm^2/s). In Fig. 5 we plotted the absolute value of the phase shift between the thermopile voltage and the heater voltage versus frequency for the two liquids. As expected, the faster liquid (water) gives the lower phase shift (delay). Looking at Fig. 5 we see that the difference between the two signals increases with the frequency. As our purpose it to relate the phase shift between U_{out} and U_h with the thermal diffusivity of the liquid sample we consider for the calibration curve only the results measured at one frequency (1 Hz). Therefore, for the construction of the calibration curve we considered the values measured at 1 Hz. At higher frequency the

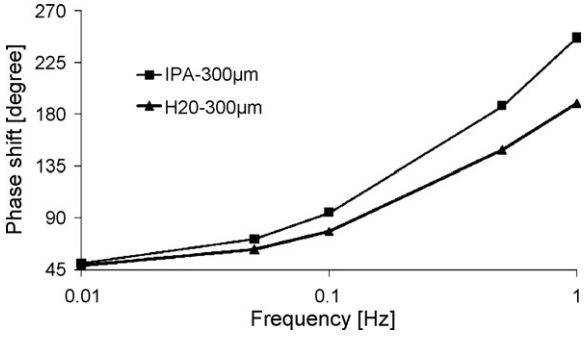

Fig. 5. Phase shift between the thermopile voltage and the heater voltage for two liquid samples (water and IPA) with a heating power of 1.5 mW_{p-p}. Measurements are done at 30 °C across a 300-μm distance.

difference between the phase shift for the two liquids will be even higher, but the amplitude of the signals become very low and the signal-to-noise ratio will be too low.

The calibration liquids we use are: demi water; IPA; methanol and water–methanol solutions at various methanol concentrations.

It is common to use reference materials with known thermal properties for the calibration. Although reference materials for calorimetry are listed in [12], there are no guidelines regarding measurements of thermal conductivity and thermal diffusivity of liquid samples. In order to perform the device calibration, we decided to use water–alcohol mixtures because they are easily available and with well-known thermal properties. Indeed, several papers [13–16] have been published about the measurement of the thermal properties of water, alcohol and water–alcohol mixtures. The IPA samples we used have a purity of 99.8% while the methanol samples have a purity of 99.5%. The demi water has a resistivity of more than 15 MΩ cm. We performed measurements in an oven at 30 °C and we used, as values for the thermal conductivity and thermal diffusivity of the liquids, the measured values reported in [13–15]. In [14,15] the values of thermal diffusivity for the water–alcohol mixtures are reported only for a temperature of 23 °C. For a change of the ambient temperature of 7 °C [15] the variation of the thermal diffusivity of the used liquid samples with the temperature is maximum of 2.5% of the value at 23 °C. We compensate for this error adding a correcting factor to the values reported in [14]. The correction factor is calculated from the difference between the values at 23 °C and the values at 30 °C reported by [15].

Using the calibration curve it is then possible to calculate the thermal properties, not listed in literature, of other liquid samples. Other liquids, as water–IPA mixture have also been measured. The thermal conductivity and thermal diffusivity values calculated with the calibration curve have been compared with the values present in literature in [11]. The results are presented in the next section.

5. Experimental results

5.1. Measurements

In this section we present the measurements performed to construct the calibration curves of the device.

The temperature of the CTS oven is set at 30 °C. The bias voltage we applied to the heater is a sinusoidal signal with amplitude of 5 V_{PP} and with frequency in the range between 10 mHz and 1 Hz. For different liquid samples we measured the amplitude of the thermopile voltage and the phase shift between the thermopile voltage and the heater voltage. Using the thermal conductivity values from [13] we made a calibration curve. In Fig. 6 we plotted the thermal conductivity of the liquid samples as function of the amplitude of the thermopile voltage at 10 mHz for a distance between heater and thermopile of 300 μm. We utilized a 2nd order polynomial to interpolate the experimental results. With a 2nd order polynomial the error is less then 4% of the experimental results. To get an error less then 0.5% it is necessary to use a 4th order polynomial. Thanks to the calibration curve is possible to calculate the thermal conductivity of liquid samples not studied yet. To prove this we compared, for IPA–water mixture at 50 weight% (wt%), the thermal diffusivity value present in [13] with the one calculated with the calibration curve. The difference between the two values is 1.2% (0.004 mW/K m) of the value present in [13], which is inside the inaccuracy of the interpolation curve. The values of thermal conductivity calculated using the calibration curve for the measured MeOH–water and IPA–water mixtures are listed in Table 2.

Table 2
Calculated values of thermal conductivity, at 30 °C, for several MeOH–water and IPA–water mixtures using the calibration curve. The maximum difference between the values in [13] and the calculated ones is 0.01 W/K m.

Sample	Calculated K [W/K m]
IPA 100%	0.151
IPA75%	0.208
IPA50%	0.308
MeOH 100%	0.199
MeOH 75%	0.250
MeOH 50%	0.340
MeOH 25%	0.470
MeOH 0%(=H_2O)	0.605

A change in the output voltage of the order of 5 mV for a change in the thermal conductivity from 0.1 to 0.6 W/K m would correspond to a sensitivity of about 11 mV/(W/K m). A resolution in thermal conductivity value is obtained in the order of 0.02 mW/K m. To calculate the resolution we used the standard deviation value, about 0.2 mV, obtained measuring the output signal three times.

The information about the thermal diffusivity is distilled from the phase shift between the thermopile voltage and the heater voltage at 1 Hz. Using the thermal diffusivity values present in literature [14–16], with the necessary correction, we made a calibration curve. Fig. 7 shows the absolute value of the phase shift at 1 Hz heating signal for a distance between heater and thermopile of 300 μm. Also in this case a 2nd order polynomial was used to interpolate the experimental results. For Methanol concentration of 75 wt% we measured a value very close to the one measured for a 100 wt% concentration. This is in agreement with the results showed in [14]. The thermal diffusivities of IPA–water mixtures (75% and 50%) shown in Fig. 7 are calculated using the calibration

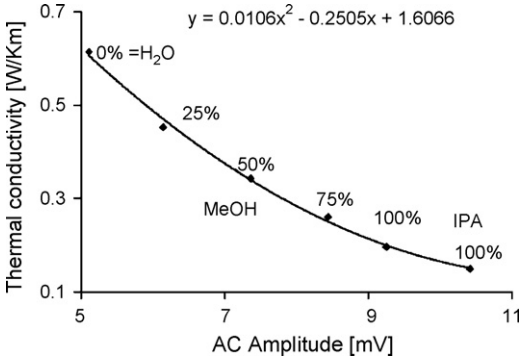

Fig. 6. Thermal conductivity of IPA and MeOH–water mixtures (100, 75, 50, 25, 0 wt%) as function of thermopile voltage at 10 mHz for 300-μm distance from the heater. Measurement performed at 30 °C.

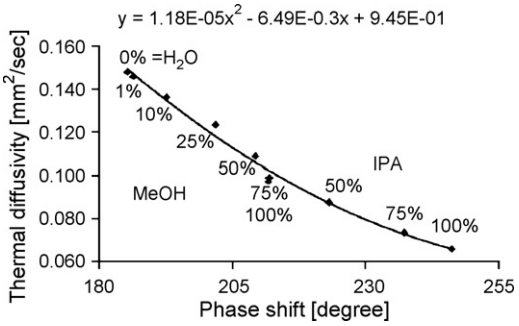

Fig. 7. Thermal diffusivity of IPA and MeOH–water mixtures (100, 75, 50, 25, 10, 1, 0 wt%) as function of thermopile voltage at 1 Hz for 300-μm distance from the heater. Measurement performed at 30 °C.

Table 3
Calculated values of thermal diffusivity, at 30 °C, for several MeOH–water and IPA–water mixtures using the calibration curve. The maximum difference between the values in [14–16], corrected for a temperature of 30 °C, and the calculated ones is 0.006 mm^2/s.

Sample	Calculated α [mm^2/s]
IPA 100%	0.067
IPA75%	0.073
IPA50%	0.088
MeOH 100%	0.103
MeOH 75%	0.102
MeOH 50%	0.106
MeOH 25%	0.118
MeOH 10%	0.135
MeOH 1%	0.147
MeOH 0%(=H_2O)	0.149

curve. Those values, together with the values of thermal diffusivity calculated for the measured MeOH–water mixtures, are presented in Table 3.

At a distance of 300 μm and at 1 Hz heating voltage, the difference in phase shift between water and IPA is approximately 55°. With a standard deviation of 0.7°, the obtained resolution is 0.001 mm^2/s.

6. Conclusions

We presented a calorimeter chips suitable for measurement of thermal conductivity and thermal diffusivity of liquid samples. For the device calibration water–alcohol mixtures at different alcohol concentrations have been used. The device we calibrated consists of two calorimeter chips glued on top of each other to form a close chamber. The chamber is intended to contain and isolate the liquid sample from the ambient. Both chips have a heater and a thermopile on the centre of a SiN membrane. When the heater is excited with an AC signal the thermopile shows an output voltage with an amplitude and phase shift related to the thermal conductivity and thermal diffusivity of the liquid sample contained inside the device chamber, respectively. Using the values of the thermal properties of the liquid samples found in literature we constructed two calibration curves for the device. The calibration curves can be used to determine the thermal conductivity and thermal diffusivity of liquid samples under test. A resolution of 0.02 mW/K m has been obtained for thermal conductivity measurements that is a value typically well below 1% of the thermal conductivity values of most liquids (usually around 200 mW/K m). For the thermal diffusivity measurements we obtained a resolution of 0.001 mm^2/s that is about 1.4% of the IPA thermal diffusivity.

Acknowledgements

The authors would like to thank Fabio Santagata for his help in the draft of the journal and for his useful suggestions. Further the authors would like to thank G. Pärr for the design of the chip and Jeroen Kool of the Vrije Universiteit of Amsterdam for the help with the liquid measurement set up. The Authors thank the European Commission for their financial support via the Marie Curie Research and Trainings Network project Cellcheck (www.cellcheck.eu) (Contract number: MRTN-CT-2006-035854).

References

[1] Y. Zhang, S. Tadigadapa, Thermal characterization of liquids and polymer films using a microcalorimeter, Applied Physics Letters 86 (2005), 034101/1–034101/3.
[2] Y. Zhang, S. Tadigadapa, Calorimetric biosensors with integrated microfluidic channels, Biosensors & Bioelectronics 19 (2004) 1733–1743.
[3] J.M. Köhler, M. Zieren, Micro flow calorimeter for thermoelectrical detection of heat of reaction in small volumes, Fresenius Journal of Analytical Chemistry 358 (1997) 683–686.
[4] M. Zieren, J.M. Köhler, A micro-fluid channel calorimeter using BiSb/Sb thin film thermopiles, in: Proc. Transducers 97, 1997, pp. 539–542.
[5] Data sheet liquid nanocalorimeters, www.xensor.nl.
[6] Y.-T. Chen, C.-W. Chang, Y.-R. Chung, J.-H. Chien, J.-S. Kuo, W.-T. Chen, P.-H. Chen, A novel CMOS sensor for measuring thermal diffusivity of liquids, Sensors and Actuators A 135 (2006) 451–457.
[7] T. Hashimoto, J. Morikawa, T. Kurihara, T. Tsuji, Frequency dependent thermal diffusivity of polymers by temperature wave analysis, Thermochimica Acta 304/305 (1997) 151–156.
[8] A.A. Minakov, S.A. Adamovsky, C. Schick, Advanced two-channel ac calorimeter for simultaneous measurements of complex heat capacity and complex thermal conductivity, Thermochimica Acta 403 (2003) 89–103.
[9] G. Pärr, E. Santagata-Iervolino, A.W. van Herwaarden, W. Wien, M.J. Vellekoop, Thermal characterization of microliter amount of liquids by a micromachined calorimetric transducer, in: Proceeding MEMS, 2009, pp. 535–538.
[10] P.J. French, P.M. Sarro, R. Mallée, E.J.M. Fakkeldij, R.F. Wolffenbuttel, Sensors and Actuators A-Physical 58 (1997) 149–157.
[11] J. Morikawa, T. Hashimoto, Simultaneous measurement of heat capacity and thermal diffusivity in solid–solid and liquid–liquid phase transitions of n-alkane, Thermochimica Acta 352/353 (2000) 291–296.
[12] R. Sabbah, An Xu-Wu, J.S. Chickos, M.L. Planas Leitão, M.V. Roux, L.A. Torres, Reference materials for calorimetry and differential thermal analysis, Thermochimica Acta 331 (1999) 93–204.
[13] M.J. Assael, E. Charitidou, W.A. Wakeham, Absolute measurements of the thermal conductivity of mixtures of alcohols with water, International Journal of Thermophysics 10 (1989) 793–803.
[14] A. Matvienko, A. Mandelis, High-precision and high-resolution measurements of thermal diffusivity and infrared emissivity of water–methanol mixtures using a pyroelectric thermal wave resonator cavity: frequency-scan approach, International Journal of Thermophysics 26 (2005) 837–854.
[15] J. Wang, M. Fiebig, Determination of the thermal diffusivity of aqueous solutions of methanol in an extended range of temperature by a laser-induced thermal grating technique, Experimental Thermal and Fluid Science 13 (1996) 38–43.
[16] A. Matvienko, A. Mandelis, Ultrahigh-resolution pyroelectric thermal-wave technique for the measurement of thermal diffusivity of low-concentration water–alcohol mixtures, Review of Scientific Instruments 76 (2005), 104901/1–104901/7.